

Recent study of the high performance confinement and the high beta plasmas on the Large Helical Devices

K.Y. Watanabe, A. Komori, H. Yamada, K. Kawahata, T. Mutoh, N. Ohyaabu, O. Kaneko, S. Imagawa, Y. Nagayama, T. Shimozuma, K. Ida, T. Mito, K. Nagaoka, R. Sakamoto, S. Ohdachi, R. Kumazawa, H. Funaba, Y. Narushima, S. Sakakibara, Y. Suzuki, T. Morisaki, S. Sudo, O. Motojima and LHD experimental Group

Author affiliations should be centered 10-point italic type National Institute for Fusion Science,322-6 Oroshi-cho, Toki 509-5292, Japan

Some topics of the recent LHD (Large Helical Device) experimental results related with the extension of the operational regime to the fusion reactor are reviewed. LHD experiments can demonstrate the high ion temperature discharge with confinement improvement similar to the internal transport barrier. Super high density and high pressure plasmas with IDB (internal diffusion barriers) are obtained. The central electron density exceeds $1.1 \times 10^{21} \text{m}^{-3}$ and IDB discharges enable good confinement regime to be extended to the high density operation regime. 5.1% volume averaged beta plasma is transiently produced by pellet fuelling and 5% plasma is maintained in quasi-steady state by gas-puff fuelling. By using an IDB, high central beta plasma comparable with standard high beta operation has been achieved. On the steady state operation, the pulse time with high input power operation is extended by the replacement of the divertor plate with good heat conductivity. The future subjects on LHD experiments to reactor are also discussed.

Keywords: Large Helical Device, recent progress, high ion temperature, internal transport barrier, super high density, internal diffusion barrier, high beta, resistive interchange, steady state, high heat load

1. Introduction

The LHD (large helical device) is the largest super-conducting helical machine in the world [1]. The experiment started at the end of the March 1998. Up to Dec. 5th 2008, 90426 discharges were done. As the typical plasma parameters, the plasma major radius is around 3.7m, the plasma volume is around 30m^3 . The maximum operational magnetic field strength is 3T. The central rotational transform is less than 0.4 and the edge rotational transform is more than 1.5. At the core, the magnetic shear is weak and at the edge, it is strong.

In this paper, we will show some topics of the recent LHD experimental results related with the extension of the operational regime to the fusion reactor. In the table 1, the recent achievement in LHD experiments and the designed targets are shown. On the central temperature, 5.2 keV at $n_e \sim 1.6 \times 10^{19} \text{m}^{-3}$ for ion and 10keV for electron are achieved. On the beta value, which is a key parameter to construct the economical fusion reactor, the volume averaged beta reaches 5.1% transiently. Steady state discharges with the 490kW input power for over 54minutes, 1.1MW for 800s are maintained. The maximum operational density exceeds 10^{21}m^{-3} in the center. The available heating power is increasing. Now more than 25MW heating power is available by NBI, ECH and ICH. As the heating power

increases, the plasma stored energy also increases. Now it exceeds 1.6GJ, which is comparable to the big tokamaks. These extension of the operational plasma parameters enable the systematic study near the fusion reactor plasmas.

This paper is organized as follows. At first, the characteristics of the high ion temperature discharges with

	Achieved	Designed Target
Central Ion Temperature	5.2keV ($1.6 \times 10^{19} \text{m}^{-3}$)	10keV ($2 \times 10^{19} \text{m}^{-3}$)
Central Electron Temperature	10keV ($0.5 \times 10^{19} \text{m}^{-3}$)	10keV ($2 \times 10^{19} \text{m}^{-3}$)
Central Density	$1.1 \times 10^{21} \text{m}^{-3}$ (0.3keV) $1 \times 10^{20} \text{m}^{-3}$ (1.5keV)	$1 \times 10^{20} \text{m}^{-3}$ (1keV)
Volume averaged β	5.1% (0.425T)	> 5% (1-2T)
Long pulse operation with high heating power	54m28s (490kW) 800s (1100kW)	1hour (3,000kW)
Fusion Triple product	$5 \times 10^{19} \text{keV} \text{m}^{-3} \text{s}$ [$n_{e0} \tau_E T_{e0}$]	$5 \times 10^{19} \text{keV} \text{m}^{-3} \text{s}$ [$\langle n_e \rangle \tau_E \langle T_e \rangle$]

Table.1 Achieved plasma parameters (up to Dec. 2008) and the designed target.

confinement improvement like ITB (Internal transport barrier) are shown. Next the high density operation with IDB (internal diffusion barrier) is mentioned. And the high beta plasma and its characteristics are shown. The steady state operation with high input power and high heat load is also mentioned. Finally we summarize the recent LHD experimental results and discuss the future subjects on LHD experiments to reactor.

2. Recent experimental results

2.1 High ion temperature discharges

In the high ion temperature (high- T_i) operation, a key issue is the updated NBI heating systems. At present, LHD has 4 beam lines of NBI system, which consists of 3 tangential beam lines and 1 perpendicular beam lines. Tangential beams are characterized high energy with negative-ion sources. Then, electrons are mainly heated. Perpendicular beam lines are updated recently [2]. It is characterized as low energy ion sources, and it is effective to heat ions. Moreover it works as a diagnostic beam for CXRS.

The productions of high- T_i plasmas with low Z_{eff} have been performed by high power NB heating in LHD with the inwardly-shifted configurations with $3.575\text{m} < R_{\text{ax}} < 3.7\text{m}$ [3]. The inward shifted configuration has a good particle confinement. A typical wave form of high- T_i discharge is shown in Fig. 1. The time evolution of the core ion and electron temperature (T_i and T_e), the heating power and the line averaged electron density are shown in Fig.1(a) and(b). At the beginning of the discharge, the target plasma was started by ECH and sequentially connected to the low power NB heating phase with P-NBI (positive NBI) alone. After superposition of N-NBIs (negative-NBIs), the central T_i and T_e significantly increases. Finally, T_i exceeds T_e (high- T_i phase). The typical density at high- T_i phase is $1\sim 2 \times 10^{19}\text{m}^{-3}$. High- T_i

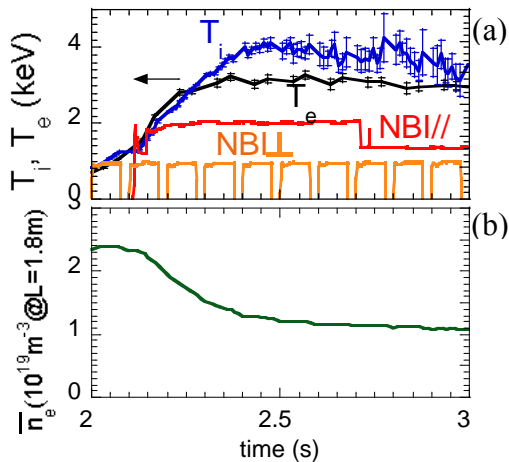


Fig.1 The time evolution of the core ion and electron temperature, the heating power and the line averaged electron density are shown in the high- T_i discharge.

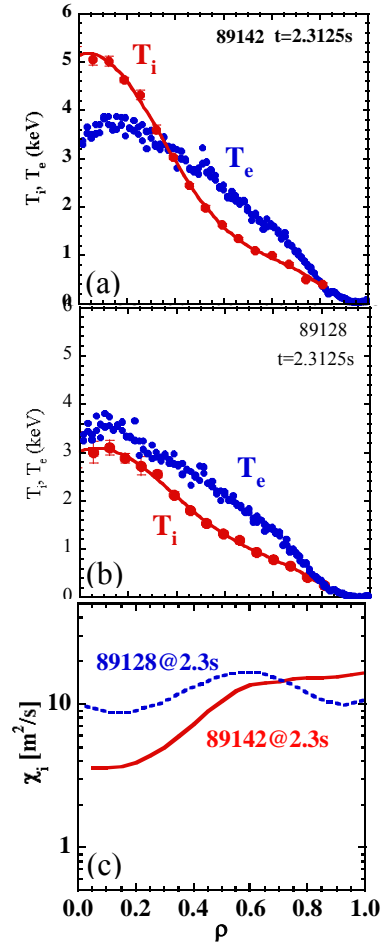


Fig.2 The typical radial profile of the T_i and T_e at the high- T_i phase (a) and the normal discharges, L-mode, (b). (c) The radial profile of the ion thermal conductivities for L-mode and high- T_i phase.

phase is maintained for 200 ms, which is almost several times longer than the energy confinement time.

Figure 2(a) shows the typical radial profile of the T_i and T_e at the high- T_i phase, where $n_e \sim 1.6 \times 10^{19}\text{m}^{-3}$. The temperature profile at the high- T_i phase is characterized as the higher T_i comparison with T_e at the center and the much steeper T_i gradient than T_e at the core, which suggests the achievement of the improved confinement with ITB formation. On the contrary, the radial temperature profile in the normal discharges (L-mode) is shown in Fig.2(b). It should be noted that ITB formation is typically observed for the larger ion heating power per the ion density comparing with the normal discharges. Figure 2(c) shows the radial profile of the ion thermal conductivities for L-mode and high- T_i phase. In the core region, the thermal transport is improved in the high- T_i phase. It should be noted that the radial electric field is negative in the ITB region according to the preliminary measurement of the electric potential by the heavy ion beam probe, which is consistent with the theoretical prediction based on the neoclassical ambipolar particle flux condition. The reduction of the anomalous part of the ion thermal

conductivity is considered more dominant on the ITB formation comparing with that of neoclassical one. The mechanism of ITB structure formation has not been understood well yet. The understanding is one of our future subjects.

2.2. High density operation

In LHD, super high density and high pressure plasmas are obtained with IDB, which is the distinguished feature because this kind of feature has not been observed in tokamaks [4,5]. Super high density is obtained just after the multi-pellet injection. And the high central pressure is obtained during the density decay phase. Maximum central density exceeds 10^{21} m^{-3} , and the maximum central pressure reaches 150kPa.

In the IDB region, the temperature profile is relatively flat and the IDB plasma is not accompanied by an improvement in thermal transport, while the temperature gradient is established in the small density region outside of IDB. The IDB plasma is characterized as the large Sharanov shift, and the large stochastic region is predicted in the large electron temperature gradient region as shown in Fig.3 according to HINT [6] calculation. However, the large degradation of the thermal transport is not observed in the predicted stochastic region.

As an advantage of the IDB discharges, it enable the plasmas to extend the good confinement to the higher density operation regime. Figure 4 shows the dependence of the stored energy on the line averaged density for the almost same heating power. In Fig.4, the open squares, the blue circles and the red circles correspond to the discharges fuelled by the gas-puff, the pellets without IDB formation and the pellets with IDB formation. In the gas-puff operations, the confinement performance degrades as the density increases. On the contrary, in the pellet operations, the good confinement performance region extends to the higher density region comparing with the gas-puff

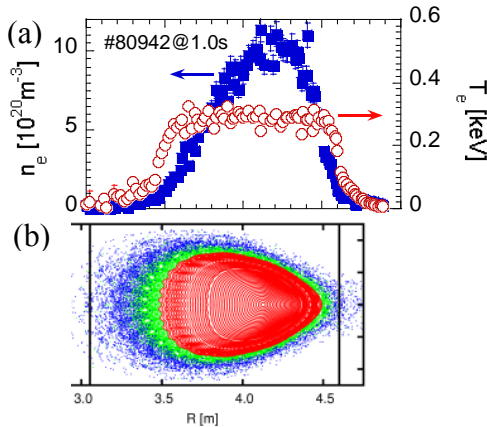


Fig.3 (a) Density and electron temperature profile of the IDB plasma with the highest central density. (b) The predicted magnetic surface structure for IDB plasma by HINT code.

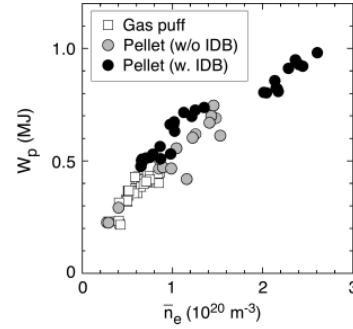


Fig.4 The plasma stored energy as the function of density for the discharges with various density profiles and by various fueling methods.

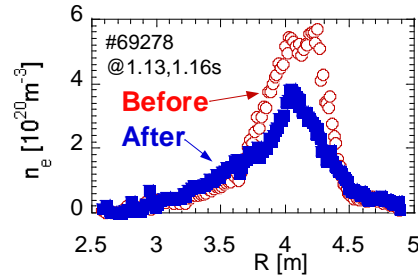


Fig.5 The density profiles just before and after a CDC event.

operations.

Next we will discuss the operational limit of the IDB plasmas. In IDB plasmas with high central pressure, the core density collapse (CDC) events are often observed [7]. Figure 5 shows the density profiles just before and after a CDC event. At the CDC event, core density is abruptly expelled. The electron temperature profiles little changes before and after a CDC event. The typical time of the collapse is $\sim 100 \mu\text{s}$, It is much shorter than that of the collapse due to the MHD instabilities in LHD, which is more than 5 ms [8, 9]. And in the collapse due to the MHD instabilities, the changes of the electron temperature profile is significant. Here it should be noted that the temperature gradient is much larger than the density gradient in the core at the conventional MHD driven collapse. Sometimes MHD events are observed around CDC events. However, the driving mechanism is not clear yet. And another limitation of IDB formation is by lack of central heating power. High density plasma inhibit NB penetration to the core. Then the density rise by pellet is limited.

2.3. High beta discharges

The high beta regime has been extended to the volume averaged diamagnetic beta $\langle \beta \rangle$ of 5% mainly by optimizing the magnetic configuration and the increase in the NBI heating power [9]. Figure 7 shows the waveform of the $\langle \beta \rangle \sim 5\%$ plasma, which corresponds to the maximum beta value. In Fig.7(a), the averaged beta value and the NBI heating power are shown and the magnetic fluctuations resonated with the edge region in Fig.7(b)-(d). Operational magnetic field strength is 0.425T. The plasma

is produced and maintained by mainly tangential NBI. Density is controlled by gas-puffing. High beta plasma near the 5% is maintained without disruption. In this discharge, the duration time near the 5% is limited for 40 times energy confinement time due to the termination of a NBI unit. If we can keep the power, the 5% beta plasma would be maintained in steady state. On the properties of the low mode number MHD activities in high beta region, only resonating mode width peripheral surfaces appear, and the core resonant MHD mode is not observed. Figure 8 shows the beta profile at $\langle\beta\rangle = 5\%$. Though some fine structures like a flattening and asymmetry in the profile appear, the effects on a global confinement look small. According to theoretical analysis for low mode number ideal and/or resistive MHD instability, only the instabilities with narrow radial mode width are predicted.

Next we discuss the effect of MHD instabilities on the confinement [10]. Figure 8(a) shows the characteristics of the local confinement properties at the edge normalized gyro-Bohm anomalous transport model. It should be noticed that ISS95 empirical confinement scaling has the similar dependence of Gyro-Bohm anomalous transport model.

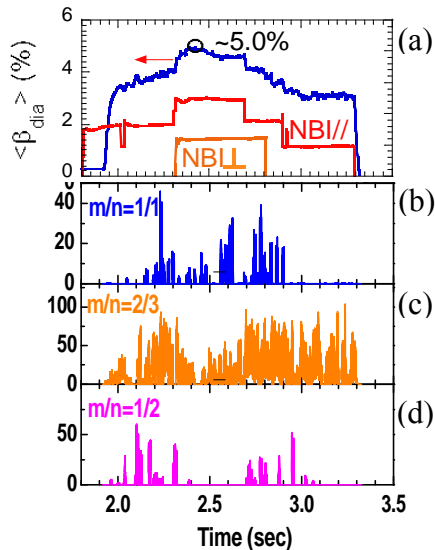


Fig.6 A waveform for the 5% volume averaged beta discharges. (a) beta value and the heating power by NBI. (b), (c) and (d) are the magnetic fluctuation with $m/n=1/1$, $2/3$ and $1/2$ mode numbers, respectively. Here m and n are the poloidal and toroidal mode numbers.

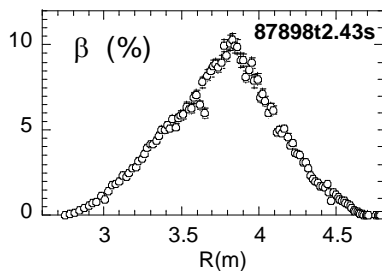


Fig.7 The beta profile evaluated by the electron density and the electron temperature, where $Z_{eff}=1$ and $T_i=T_e$ are assumed.

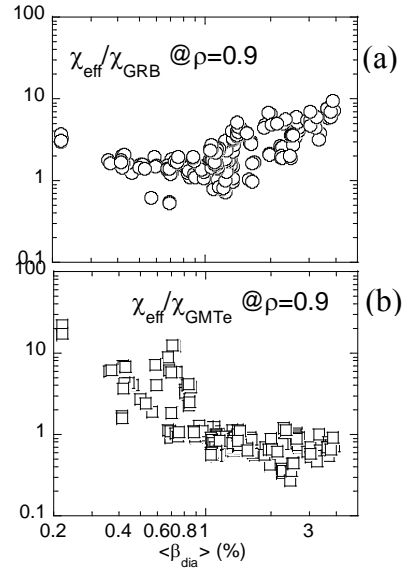


Fig.8 The normalized peripheral thermal transport coefficients as the function of the beta value (a) by the gyro-Bohm anomalous model and (b) the resistive interchange mode driven turbulence.

The local confinement performance at the edge gradually degrade as beta increases. Figure 8(b) shows the peripheral transport properties normalized by a resistive interchange mode driven turbulence proposed by Dr. Carreras et al [11]. In high beta region, the beta dependence of experiment data is well reproduced by that, which suggests the resistive interchange mode make a important roll on the local transport properties in edge region. In the resistive MHD instability, the magnetic Reynolds number, S is a key parameter and the anomalous transport driven by it would decrease as S increases. The S is proportional to the cubic of the magnetic field strength under a scaling. If we can obtain 4% beta discharges in 1T, the S is expected 10 times larger than the present 5% beta plasmas. To confirm the influence of the resistive interchange mode turbulence driven transport by the extension of the magnetic field, we need to extend the high beta regime to the operations with the higher magnetic field.

Recently another high beta plasma production is established by using an IDB scenario with the multiple pellet injections [7]. As the magnetic field strength decreases, CDC effect in IDB discharges on confinement

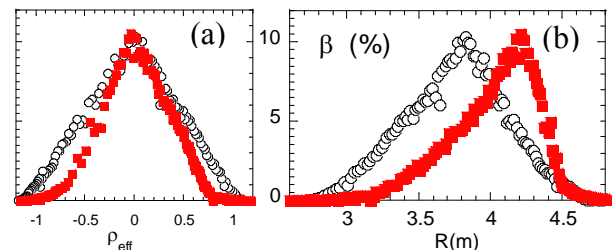


Fig.9 The beta profile as the function of the normalized minor radius (a) and the major radius (b) for the IDB discharge (close squares) and the standard high beta discharge (open circles).

becomes small. Then in low field operation with IDB plasmas, high central beta plasma comparable with standard high beta operation has been achieved. The beta profiles are shown as a function of the normalized minor radius in Fig.9(a) and of the major radius in Fig.9(b). In Fig.9, the closed circles denotes the beta profiles produced by IDB scenario and the open circles by the standard high beta scenario, which is exactly same with Fig.7. $\beta_0 \sim 10\%$ is transiently achieved under $\langle \beta \rangle \sim 3\%$, which is comparable to that of the standard high beta operation with $\langle \beta \rangle \sim 5\%$. The beta profiles by the IDB scenario is characterized as the steeper gradient of beta in the core comparison with that in the edge and the larger Shafranov shift. The production of the peaked pressure profile has the advantage for the MHD stability because of the large Shafranov shift and the steep pressure gradient and for the high fusion power output because it is proportional to the square of beta value not to the beta value itself.

2.4. Steady state operation

In LHD long pulse discharges, the extension of the duration time of discharges with the high heating power after the achievement of the world record of the largest heating energy (integrating heating power). The long pulse discharges with the high heating power is considered useful for a progress of the investigation on the impurity transport, the plasma-wall interaction and so on, characteristic time scales of which are long, because the discharges with the higher heating power have closer performance to the reactor. Recently the pulse time with high input power operation is extended by the replacement of the divertor plate and a model of the upper limit of the duration time of the long pulse discharges against the heating power based on the accumulated experimental data [12].

The duration times of the discharges, τ_{pl} are shown as a function of the heating power, P_H in Fig.10. The open circles corresponds to the experimental data before the replacement of the improved divertor plates with good heat conductivity, and the closed squares to ones after the replacement. The duration time data of the discharges before the replacement of the divertor plates were obtained for the wide range of heating power, which suggests the existence of a limitation of τ_{pl} . The envelope of the maximum of τ_{pl} is approximately expressed by the solid curve shown in Fig.10 and by the following equation:

$$\tau_{pl} \propto \log(P_H / (P_H - P_c)), \quad (1)$$

which corresponds to empirical scaling law of the τ_{pl} against the heating power. In eq.(1), P_c is a constant. In Fig.10, the dashed line corresponds to the contour of the integrated heating power. From the solid line and the

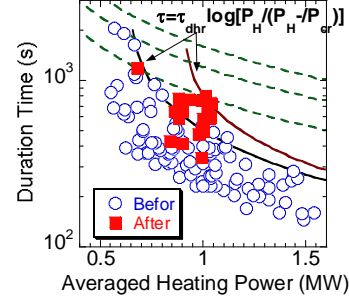


Fig.10 The duration times of the discharges, τ_{pl} as a function of the heating power, P_H . The open circles corresponds to the data before the replacement of the improved divertor plates, and the closed squares to ones after the replacement.

dashed lines, the larger integrated heating power discharges are easily obtained in the lower input power discharges for LHD. The empirical scaling law of the τ_{pl} is consistent with the following model. The upper limit of the temperature of the divertor plate, T_{div-cr} is assumed to keep the discharges stationary for long time. And the temperature of the divertor plate is determined by its time constant of the heat removal, τ_{dhr} , where the saturated temperature is assumed proportional to heating power, P_H and the τ_{dhr} . The strong correlation between the temperature of the divertor plate and the penetration of the high Z impurity to the bulk plasma from the divertor plate is observed in the LHD long pulse discharges up to date [12]. Under the above assumption, the predicted duration times of the discharges is expressed as

$$\tau_{pl-pre} = \tau_{dhr} \log(P_H / (P_H - P_{cr})). \quad (2)$$

Here $P_{cr} = T_{div-cr} / C \tau_{dhr}$ and C is a constant depending on the magnetic configurations, the plasma parameters and the heating methods. Eq.(2) coincides the empirical scaling based on the LHD experiments and it suggested the improvement of the heat conductivity of the divertor plate is the most important critical issue to extend the duration time of the discharges with the high heating power. As shown by the black squares in Fig.12, the duration time of the discharges with high heating power is extended after the replacement of the improved divertor plates with good heat conductivity: from 400s to 800s for the discharges with 1MW heating power, where the high central electron temperature with 1.5keV at $n_e = 0.6 \times 10^{19} \text{ m}^{-3}$ is maintained. From Fig.10 and Eq.(2), it is speculated that the replacement of the divertor plate improve the capability of the heat removal by ~ 1.4 times as the time constant of the heat removal.

3. Summary and discussion

In this paper, the recent progress of the LHD experimental results related with the extension of the operational regime to the fusion reactor is reviewed.

LHD experiments can demonstrate the high ion

temperature discharge with confinement improvement similar to Internal Transport Barrier (ITB), which is characterized as the higher T_i comparison with T_e at the center and the much steeper T_i gradient than T_e at the core. In the LHD, super high density and high pressure plasmas with internal diffusion barriers are obtained, which is the distinguished feature because this kind of feature has not been observed in tokamaks. The central electron density exceeds $1.1 \times 10^{21} \text{m}^{-3}$ and IDB discharges enable good confinement regime to be extended to the high density operation regime more than several 10^{20}m^{-3} . 5.1% volume averaged beta plasma is transiently produced by pellet fuelling and 5% plasma is maintained in quasi-steady state by gas-puff fuelling. Up to 5% beta, disruptive phenomena is not observed. However, the gradual degradation of the energy confinement is observed with beta value, which would result in the enhancement of the resistive interchange mode turbulence due to the small magnetic Reynolds discharges. By using an IDB, high central beta plasma comparable with standard high beta operation has been achieved. On the steady state operation, the pulse time with high input power operation is extended by the replacement of the divertor plate with good heat conductivity: from 400s to 800s for the discharges with 1.1MW heating power. A model of the upper limit of the duration time of the long pulse discharges against the heating power based on the accumulated experimental data is established. According to the model, the heating energy would extend to 2000s when the heating power is 0.9MW.

Finally we discuss the subjects on LHD experiments to the reactor. At present, for LHD type reactor, 2 operation scenarios are considered; high temperature scenario and high density scenario. High temperature scenario is a conventional scenario. In principle, LHD target parameters as shown in table I were designed based on the high temperature scenario. As the subjects to high temperature scenario, the following items are picked up. (1) reduction of neoclassical transport in low collisional regime. In order to demonstrate it, the achievement of the positive electric field in the low collisional regime, the so-called "electron root in the n-regime" and the improvement of the ion thermal transport are necessary. Moreover, the high performance confinement comparing with the ISS95 scaling in low collisionality and high beta regime under low beam pressure should be demonstrated because the present high beta discharges are obtained only in the relatively high collisionality regime and under the non-negligible beam pressure, and their confinement properties are poorer with the higher collisionality, which is equivalent to the higher magnetic Reynolds number. In high beta regime around 5%, the beam ratio to diamagnetic energy is estimated $\sim 30\%$. LHD high beta discharges are operated at the relatively low density and low magnetic

field, and the tangential high energy particles have good confinement properties even in low magnetic field. That is the why the beam contribution is fairly large in LHD high beta discharges. The effect on MHD instabilities and equilibrium should be investigated. After discovery of the super high density operation with IDB plasmas, the high density scenario is proposed and its capabilities have been investigated [4]. As the subjects to high density scenario, the following items are picked up; (1) development of particle fuelling method in the core with high density and relatively high temperature repeatedly. (2) understandings of CDC mechanism to avoid it. (3) study of transport property in stochastic regime. As the subjects related with steady state operation, the following items are picked up; (1) study of impurity transport. (2) development of suppression method of heat load to divertor. These subjects are common for the above 2 scenario.

References

- [1] A. Iiyoshi *et al.*, Nucl. Fusion **39**, 1245 (1999).
- [2] Y. Takeiri *et al.*, Plasma Fusion Res. **3**, S1001 (2008).
- [3] K. Nagaoka *et al.*, 22nd IAEA Conf. on Fusion Energy (Geneva, 2008) EX/8-2Ra.
- [4] N. Ohyaibu *et al.*, 21st IAEA Conf. on Fusion Energy (Chengdu, 2006) EX/8-1.
- [5] R. Sakamoto *et al.*, 22nd IAEA Conf. on Fusion Energy (Geneva, 2008) EX/8-1Ra.
- [6] K. Harafuji, T. Hayashi and T. Sato, J. Comput. Phys. **81**, 169 (1989)
- [7] S. Ohdachi *et al.*, 22nd IAEA Conf. on Fusion Energy (Geneva, 2008) EX/8-1Rb.
- [8] S. Ohdachi *et al.*, 21st IAEA Conf. on Fusion Energy (Chengdu, 2006) EX/P8-15.
- [9] S. Sakakibara *et al.*, 21st IAEA Conf. on Fusion Energy (Chengdu, 2006) EX/7-5.
- [10] H. Funaba *et al.*, Plasma Fusion Res. **3**, 022 (2008).
- [11] B.A. Carreras and P.H. Diamond, Phys. Fluids B **1**, 1011 (1989).
- [12] R. Kumazawa *et al.*, 22nd IAEA Conf. on Fusion Energy (Geneva, 2008) EX/P6-29.
- [13] O. Mitarai *et al.*, 22nd IAEA Conf. on Fusion Energy (Geneva, 2008) FT/P3-19.